AIChE

Intensification of Liquid–Liquid Two-Phase Mass Transfer by Gas Agitation in a Microchannel

Yuanhai Su
Dalian Institute of Chemical Physics, Chinese Academy of Sciences, Dalian 116023, China, and
Graduate University, Chinese Academy of Sciences, Beijing 100049, China

Guangwen Chen, Yuchao Zhao, and Quan Yuan
Dalian National Laboratory for Clean Energy, and Dalian Institute of Chemical Physics,
Chinese Academy of Sciences, Dalian 116023, China

DOI 10.1002/aic.11787

In this experiment, the inert gas is used to agitate two immiscible fluids in microchannels. The mass transfer performances with or without gas agitation are investigated. 30% TBP (in kerosene)-acetic acid-water is chosen as testing system, and nitrogen as agitating gas. The superficial velocities of the immiscible liquid–liquid two phases and gas phase are varied in the range from 0.02 to 1.2 m/s, and 0 to 3.0 m/s, respectively. In microchannels, with enough gas agitating intensity, high dispersion between two immiscible liquid phases can be obtained. The overall volumetric mean mass transfer coefficients are two-folds higher than those without gas agitating, which are in the range of 3.8–30.6 s^{-1}. Some parameters which impact on the mass transfer process, such as the mixture superficial velocity of the immiscible liquid–liquid two phases, the gas superficial velocity, the microchannel structure, the gas inlet locations and the sampling time are experimentally investigated. © 2009 *American Institute of Chemical Engineers* AIChE J, 55: 1948–1958, 2009
Keywords: micromixing, microchannel, gas agitation, microreactor, interfacial area

Introduction

Among the various chemical reactions occurring in broad range of industrial application areas, multiphase reaction processes are well-known and widespread, such as gas–liquid, liquid–liquid, solid–liquid, gas–liquid–liquid three-phase reactions, etc. And these processes are determined by reaction intrinsic kinetics or mass transfer depending on the characteristics of reaction and fluid hydrodynamics. Unique features due to extremely large surface-to-volume ratio and the short transport path in microreactors,[1–3] such as fast mixing, rapid heat exchange, etc. can be used for the controlling of extreme reactions in chemical industry. The gas–liquid two-phase reaction in microreactor mostly focuses on direct fluorination,[4] hydrogenation,[5] oxidation,[6] gas absorption.[7] The liquid–liquid two-phase reaction in microreactor mostly focuses on nitration,[8] diazo-reaction,[9] nanoparticles synthesis,[10] extraction.[11] For the optimization of microchemical devices, the mass transfer characteristics inside the devices must be systematically investigated.

Some authors[12,13] have investigated homogeneous fluids mixing processes in T-shaped and twisted microchannels, respectively. Experimental and numerical results showed that ideal mixing can be obtained dependent of the asymmetrical flow conditions, the generation of vortices and secondary flow at the T-junction.[11] And the swaying of the fluids in the twisted microchannel caused chaotic advection, hence improved mixing.[12] Yang et al.[14] designed an ultrasonic

---

Correspondence concerning this article should be addressed to G. Chen at gwchen@dicp.ac.cn

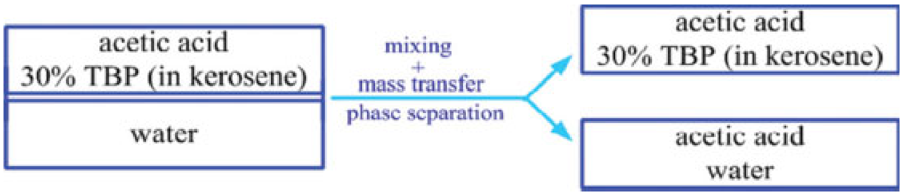

Figure 1. Schematic diagram of mass transfer process.

[Color figure can be viewed in the online issue, which is available at www.interscience.wiley.com.]

stirring microfluidic mixer, which intensified mixing by introducing ultrasonic vibration. Ismagilov et al.[15,16] investigated rapidly mixing of multiple reagents isolated in droplets (plugs), and they considered that winding microchannels make chaotic advection appear in plugs by internal circulation, which can stretch and fold the fluids striation, eventually the intensification of mixing in droplets can be obtained. Matsuyama et al.[17] demonstrated experimentally that the two miscible liquids slug droplets could be formed by introducing the immisicible carrier phase, and showed this slug-based microfluidics could offer rapid mixing and the reactant arrangements by internal circulation in slug. Jensen and his co-workers[18–20] testified that the two miscible liquids slug droplets could be formed by introducing gas in microchannel. Reactions in droplets[21,22] in microfluidic channels have also attracted many researchers due to the elimination of Taylor dispersion by internal circulation, such as the measurement of fast reaction kinetics parameters,[23] protein crystallization,[24] synthesis of nanoparticles,[25] etc. However, little attention had been paid to the immiscible liquid–liquid two-phase mixing in microchannels.

Triplett et al.[26,27] investigated the gas–liquid two-phase flow patterns in microchannels. They observed five flow patterns including bubbly, churn, slug, slug-annular and annular, and predicted the frictional pressure drop accurately by using the two-phase friction factor based on homogeneous mixture assumption. Yue et al.[28] studied the hydrodynamics and mass transfer characteristics on gas–liquid flow in a

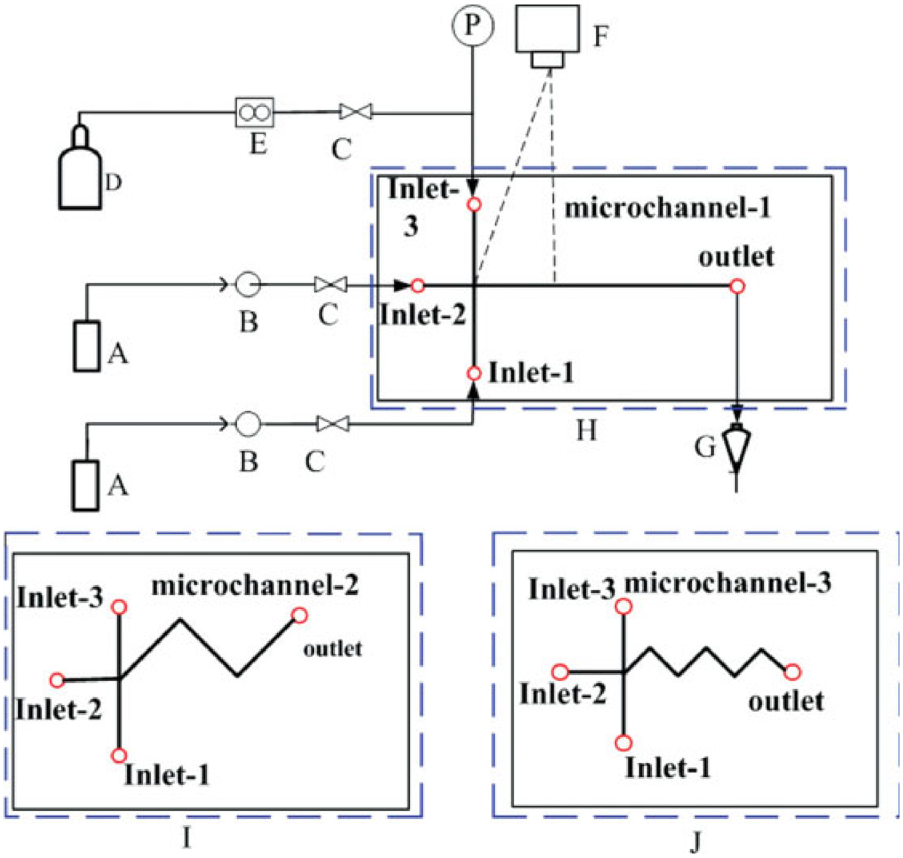

Figure 2. Schematic diagram of experimental setup.

(A) Liquid tank; (B) piston pump; (C) check valve; (D) gas cylinder; (E) mass flow controller; (F) CCD; (G) separatory funnel; (H) microchannel-1; (I) microchannel-2; (J) microchannel-3. [Color figure can be viewed in the online issue, which is available at www.interscience.wiley.com.]

Table 1. The Properties of the Working System (At 293K and Atmospheric Pressure)

Mass Transfer System	Density (kg/m^3)	Viscosity (mPa·s)	Contact Angle with PMMA (°)
Deionized water	991.4	1.05	76
30%TBP(in kerosene)	845.0	2.09	0
Nitrogen	1.16	0.017	–
30% TBP (in kerosene)/acetic acid/water system partition coefficient			0.54
30% TBP (in kerosene)-water system interfacial tension (mN/m)			9.95

rectangular microchannel. Liquid side volumetric mass transfer coefficients increased with increasing superficial liquid or gas velocity, and were higher at least one or two orders of magnitude than those in conventional gas–liquid contactors.

Zhao et al.[29,30] studied the immiscible liquid–liquid two-phase flow patterns and the mass transfer characteristics of immiscible fluids in T-junction microchannels. Five flow patterns were identified in a microchannel according to competition between interfacial tension and inertia force. The overall volumetric mass transfer coefficients were two or three orders of magnitude higher than those of conventional liquid–liquid contactors. However, they didn't consider introducing the immisicible carrier phase which can further intensify liquid–liquid mass transfer process in microchannels.

Galkin et al.[31] found that the efficiency of conventional extraction columns with sieve plates were inadequate. The extraction efficiency was nearly three times of that of conventional columns when air was introduced into the column at the lower end. Sohn et al.[32] studied a novel solvent extraction process in which the emulsion was generated by bottom gas injection rather than mechanical stirring. They claimed that the process could provide sufficiently large interfacial area for mass transfer, and had a number of advantages over the mixer-settler unit or the spray column. Lu et al.[33] carried out experimental investigation and simulation of a gas-agitated sieve plate column. They found that the overall plate extraction increased with the increasing gas velocity, and the plate numbers of gas-agitated sieve plate extraction column were 30–40% less than that of liquid–liquid sieve plate column.

It is difficult to carry out mechanical stirring in microstructured equipments, so we need to consider other methods in order to further intensify the mass transfer of two immiscible liquid–liquid two phases. In this article, the main objective is to study the effect of gas agitation on the liquid–liquid two-phase mass transfer process in microchannel. The effects of the microchannel structure, the gas flux and the gas inlet locations on the overall volumetric mean mass transfer coefficients are investigated experimentally. Mutually saturated deionized water and 30% TBP (in kerosene) are used as the working fluids (TBP is the abbreviation of tributyl phosphate), the acetic acid as the only diffusing species is transferred from oil to aqueous phase. Nitrogen is used as agitating gas. The mass transfer process between the immiscible liquid–liquid two phases is shown in Figure 1.

Experimental Section

The experimental apparatus is shown in Figure 2. The depth, width and length of three rectangular microchannels are 0.3, 0.5, and 60 mm, respectively. Microchannel-1 is straight channel, microchannel-2 has two 90° bends, microchannel-3 has five 90° bends. These microchannels are fabricated in the polymethyl methacrylate (PMMA) substrate by micromachining technology. The physical properties of the two immiscible liquid phases and nitrogen are listed in Table 1.

Flow patterns are recorded with the high-speed CCD camera. The working fluids are kerosene and de-ionized water with minute amounts of methylene blue dissolved in it for better visualization of the flow phenomena. The organic and aqueous phases are forced to flow through the horizontal rectangular microchannel by high precision piston pumps (Beijing Satellite Manufacturing Factory, measurement range: 0.01–20 ml/min). A mass flow controller (Beijing Sevenstar Electronics Company, measurement range: 0–50 ml/min) is used to ensure a constant gas flux into the microchannel.

In all mass transfer experimental runs, the volume flux ratio of organic phase to aqueous phase (defined as q) is adjusted to 1/3. When investigating the effect of microchannel structure on mass transfer, the inlet-1 and the inlet-2 are used as the inlets for the organic phase and the aqueous phase respectively, the inlet-3 is closed. Nitrogen is introduced into microchannel from the inlet-2 or the inlet-3, and directly emitted in the outlet of microchannel. Separatory funnel is used to collect samples of the outlet streams, and the two immiscible phases are separated immediately after sampling finish. The amount of acetic acid transferred from the organic phase into the aqueous phase is analyzed by neutralization titration. Each experimental run is repeated at least two times, and each data point represents the mean value of at least two measurements of the outlet concentration of organic phase, and the relative deviation does not exceed ±5% in all the experiments.

Results and Discussion

The overall volumetric mean mass transfer coefficients (ka) are used to represent the mass transfer characteristics in microchannels in this article. The Reynolds number of the two immiscible phases (Re_{M}) was used as a main parameter based on the pseudo-homogeneous model according to the main mass transfer zone at the T-junction of microchannel system.[30] In this work, based on experimental facts, the parallel flow of the immiscible liquid–liquid two phases (continuous phase flow pattern) can be transformed into the dispersed flow pattern, and better mixing performance can be obtained easily in microchannels by gas agitation, which can be considered a pseudo-homogeneous state. So, we think the pseudo-homogeneous model is suitable for explaining experimental results. The cross-sectional area of the three microchannels is a constant (0.3×0.5 mm^2), so there is a linear relationship between volume flow rate and superficial velocity. And the Reynolds numbers of the two immiscible phases can be calculated by the following equations:

$$Re_{\mathrm{M}} = \frac{D_{\mathrm{H}} U_{\mathrm{M}} \rho_{\mathrm{M}}}{\mu_{\mathrm{M}}} \tag{1}$$

$$D_{\mathrm{H}} = \frac{4A}{2(h+w)} \tag{2}$$

$$U_{\mathrm{aq}} = \frac{Q_{\mathrm{aq}}}{A} \tag{3}$$

$$U_{\mathrm{or}} = \frac{Q_{\mathrm{or}}}{A} \tag{4}$$

$$U_{\mathrm{M}} = U_{\mathrm{aq}} + U_{\mathrm{or}} \tag{5}$$

$$\rho_{\mathrm{M}} = \left(\frac{\varphi_{\mathrm{or}}}{\rho_{\mathrm{or}}} + \frac{1-\varphi_{\mathrm{or}}}{\rho_{\mathrm{aq}}} \right)^{-1} \tag{6}$$

$$\mu_{\mathrm{M}} = \left(\frac{\varphi_{\mathrm{or}}}{\mu_{\mathrm{or}}} + \frac{1-\varphi_{\mathrm{or}}}{\mu_{\mathrm{aq}}} \right)^{-1} \tag{7}$$

$$\varphi_{\mathrm{or}} = \frac{Q_{\mathrm{or}}}{Q_{\mathrm{or}} + Q_{\mathrm{aq}}} \tag{8}$$

The gas superficial velocity U_{g} is calculated using the gas density under the local pressure in the observation window by assuming a linear pressure distribution along the microchannel. The Reynolds numbers of the gas phase can be calculated by the following equations:

$$U_{\mathrm{g}} = \frac{Q_{\mathrm{g}}}{A} \tag{9}$$

$$Re_{\mathrm{g}} = \frac{D_{\mathrm{H}} U_{\mathrm{g}} \rho_{\mathrm{g}}}{\mu_{\mathrm{g}}} \tag{10}$$

The overall volumetric mean mass transfer coefficients can be calculated by the following equations:

$$R = Q_{\mathrm{or}}(C_{\mathrm{or},i} - C_{\mathrm{or},o}) = k_{\mathrm{a}} V \Delta C_{\mathrm{m}} \tag{11}$$

$$k_{\mathrm{a}} = \frac{Q_{\mathrm{or}}(C_{\mathrm{or},i} - C_{\mathrm{or},o})}{V \Delta C_{\mathrm{m}}} \tag{12}$$

$$\Delta C_{\mathrm{m}} = \frac{(C_{\mathrm{or},i} - C^{*}_{\mathrm{or},i}) - (C_{\mathrm{or},o} - C^{*}_{\mathrm{or},o})}{\ln\left[\frac{(C_{\mathrm{or},i} - C^{*}_{\mathrm{or},i})}{(C_{\mathrm{or},o} - C^{*}_{\mathrm{or},o})}\right]} \tag{13}$$

$$C^{*}_{\mathrm{or}} = mC_{\mathrm{aq}} \tag{14}$$

where a, V, Q_{or}, R, and ΔC_{m} are the interfacial mass transfer area between the phases per unit volume of the microchannel, microchannel volume, volumetric flow rate of organic solutions, extraction rates, and logarithmic mean concentration driving force, respectively. $C^{*}_{\mathrm{or},i}$ is the equilibrium concentration of the solutes in the inlet organic phase, corresponding to the actual inlet concentration of the solutes in the aqueous phase, and $C^{*}_{\mathrm{or},o}$ is the equilibrium concentration of the solutes in the outlet organic phase, corresponding to the actual outlet concentration of the solutes in the aqueous phase.

Effect of the introducing gas on the dispersion of aqueous and organic phases

The PMMA surface is hydrophobic, so the contact angle of organic phase and wall surface is smaller than that of aqueous phase, and the aqueous phase is prone to form dispersed phase.[34] In the operating range of the total liquid phase flux in all experimental runs, the organic phase and the aqueous phase form parallel flow without introducing gas. In fact, in microscale space, surface effects become obvious, and interfacial tension plays an important role.[29] Parallel flow exists over a wide range of phase flow rates in microchannel, which may be resulted from the mutual action of interfacial force and viscous force.[35]

Figure 3 shows the aqueous phase is dispersed by the gas agitation and interfacial force at the fluids inlet locations of microchannel-1 under different flux conditions. The gas agitation can break the stable parallel flow patterns of immiscible liquid–liquid two phases. At low total liquid flux and low liquid flux ratio (q=1/3), an interesting phenomenon appears as shown in Figure 3a, pearl-necklace state can be formed at the fluids inlet locations by introducing gas, in which the aqueous phase slugs and the gas slugs contact each other alternately and form a train surrounded by the organic phase. At the same superficial liquid velocity, the dispersing method may be different depending on different superficial gas velocity, at low gas velocity, the aqueous phase is sheared (Figure 3b, c), but at high gas velocity, the aqueous phase is ripped up (Figure 3d).

Figures 4 and 5 show the flow patterns change with the increase in gas superficial velocity in the microchannel-1, which are fully developed flow patterns. The immiscible liquid–liquid two phases form stable parallel flow without introducing gas into the microchannel (Figures 4a and 5a). The increase in gas velocity at the same total liquid velocity leads to shorter aqueous phase slugs and longer gas phase slugs. As the gas velocity further increases, the distance between the two adjacent gas phase slugs becomes shorter and the aqueous phase slug volume is smaller (Figures 4d and 5d). When the gas velocity is large enough, the gas occupies most of space in the microchannel and the two liquid phases are squeezed to the walls of microchannel (Figures 4e, f and 5e, f). At the moment, the inertia force of gas dominates compared to the interfacial tension of liquid–liquid two phases, the aqueous phase is broken up to smaller droplets whose size is about 10–20 μm, and even less than the minimal detection range of the high-speed CCD camera (Figure 4f). Under this operational condition, the immiscible liquid–liquid two phase mix acutely, its interface is difficult to distinguish and interfacial area is very large. In the case of low liquid flux ratio (q = 1/3), the gas–liquid–liquid three-phase flow pattern with enough gas agitation resembles the churn flow of gas–liquid two-phase in microchannel (Figure 5e, f), the interfacial area and the intensity of interface turbulence is large.

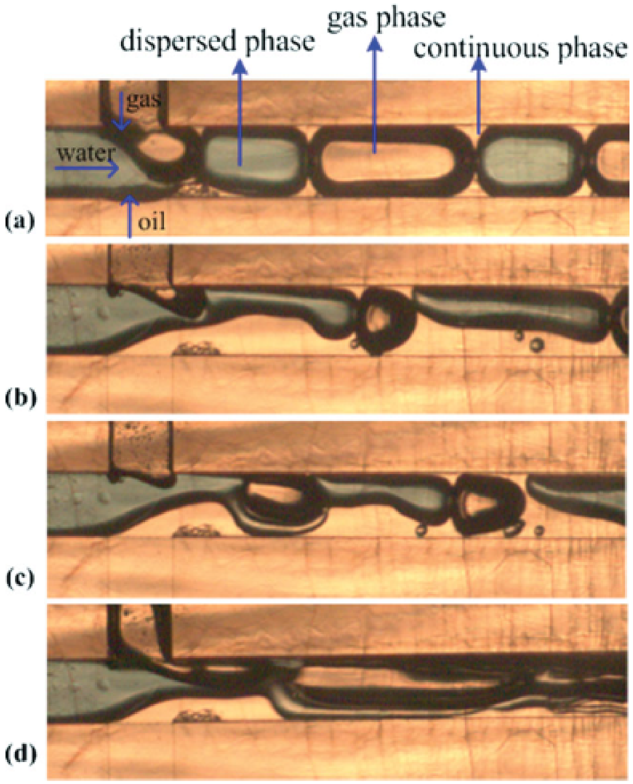

Figure 3. Effect of the gas phase shear on dispersing dispersed phase in the microchannel-1 inlet locations.

(a) $U_{or} = 0.011$ m/s, $U_{aq} = 0.033$ m/s, $q = 1/3$, $Re_M = 12.7$, $U_g = 0.144$ m/s. (b) $U_{or} = U_{aq} = 0.222$ m/s, $q = 1$, $Re_M = 109$, $U_g = 0.066$ m/s. (c) $U_{or} = U_{aq} = 0.222$ m/s, $q = 1$, $Re_M = 109$, $U_g = 0.137$ m/s. (d) $U_{or} = U_{aq} = 0.222$ m/s, $q = 1$, $Re_M = 109$, $U_g = 2.22$ m/s.

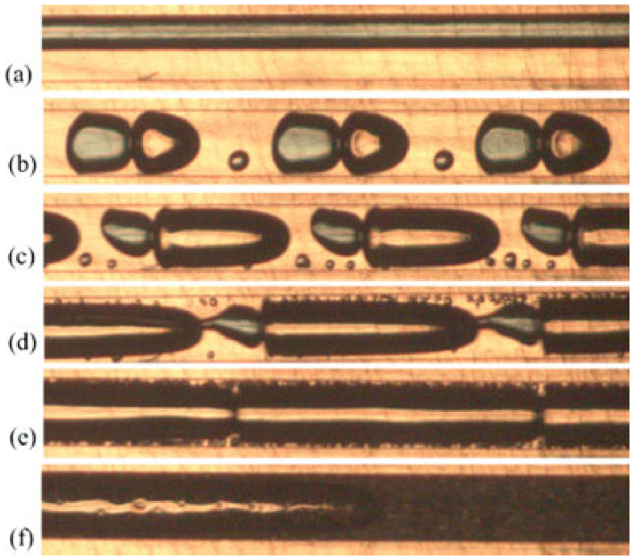

Figure 4. Effect of the gas phase flux on the dispersion of aqueous and organic phases.

$U_{or} = 0.222$ m/s, $U_{aq} = 0.111$ m/s, $q = 2$, $Re_M = 72.6$. U_g (m/s): (a) 0, (b) 0.134, (c) 0.945, (d) 1.41, (e) 2.29, (f) 2.84.

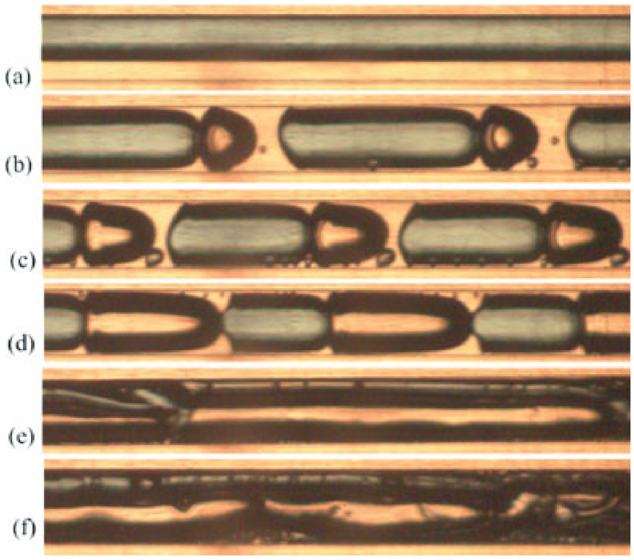

Figure 5. Effect of the gas phase flux on the dispersion of aqueous and organic phases.

$U_{or} = 0.111$ m/s, $U_{aq} = 0.333$ m/s, $q = 1/3$, $Re_M = 127$. U_g (m/s): (a) 0, (b) 0.066, (c) 0.14, (d) 0.94, (e) 3.29, (f) 4.34.

Effect of the microchannel structure on the values of ka

Microchannel structure can affect flow state and mass transfer process. Fries et al.[36] had demonstrated that for segmented gas-liquid flow, an increase in mass transfer over the complete channel diameter is possible by using meandering microchannels. Figure 6 shows the overall volumetric mean mass transfer coefficients increase with increasing of Re_M numbers in three different microchannels without introducing gas. Such a behavior is the consequence of increases in the surface renewal velocity and the interfacial mass transfer area due to the interface disturbance of the two immiscible

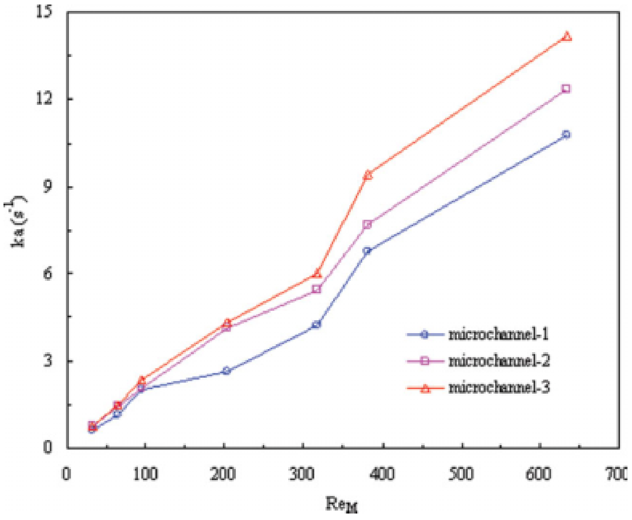

Figure 6. Effect of the microchannel structure on *ka* without gas agitation.

[Color figure can be viewed in the online issue, which is available at www.interscience.wiley.com.]

phases. At low Re_M ($Re_M < 100$), the overall volumetric mean mass transfer coefficients in the three different microchannels are nearly equal to each other, and when $Re_M > 100$, $ka_3 > ka_2 > ka_1$, especially when $Re_M > 400$, the case is more obvious. It demonstrates that the microchannel structure does not affect the mass transfer process when Re_M is relatively low, but the influence is visible with Re_M increasing. An explanation for this phenomenon may be as follows: at low Re_M numbers, the liquid–liquid two-phase flow pattern is stable parallel flow and the interface of the two phases is smooth, even in the microchannel with existing bends; however, the interface of the two immiscible fluids are stretched, folded and distorted, even secondary flow can appear when the fluids flow through the microchannel bends at medium and high Re_M numbers. Secondary flow[12] can be obtained where there are some discontinuities in the flow conduit, such as the presence of a sharp bend where centrifugal forces appear. Secondary flow causes vortices and engulfment flow. The vortices shear striation layers, and the interfacial mass transfer area increases and the mass transfer distance becomes shorter. So the mass transfer process can be dramatically intensified.

Secondary flow becomes weak and disappears quickly after flowing through the bends due to the viscous channel wall friction, but maybe appears again when meeting the next bend. Because the microchannel-3 has maximum bends (90°), hence the mass transfer is better.

Effect of the gas superficial velocity on the values of ka

Figure 7 shows the effect of the gas superficial velocity on the overall volumetric mean mass transfer coefficients. The values of *ka* increase as the gas velocity increases in the three different microchannels under different total liquid phase flux conditions. In the scope of all Re_M numbers of the experiment, the flow pattern of the immiscible liquid–liquid two phases in the microchannels is parallel flow[29] without introducing gas, but the gas can destroy the parallel flow as discussed in the front part. At low total liquid phase flux, the aqueous phase can be broken up to slugs by a litter gas agitation at the inlet locations of microchannel. There are internal circulations in slugs due to the difference in the direction of motion of the fluid relative to the walls,[15] hence the surface renewal velocity is enlarged, and the mass transfer process is intensified. As the gas velocity further increases, the volume of the aqueous phase slugs surrounded by the organic phase becomes smaller, which makes the intensity of internal circulations more dramatic and interfacial area larger, and the surface renewal velocity and the interfacial mass transfer area are further increased. The two liquid phases are squeezed to the walls of microchannel, the interface of the immiscible liquid–liquid two phases is not explicit and the disturbance is drastic with enough gas agitation, which all increase the interfacial mass transfer area and the surface renewal velocity, and finally large overall volumetric mean mass transfer coefficients can be obtained.

In fact, in microscale space, the microchannel can be considered as microstirred tank, and the gas as microagitator, that is, as a way of introducing exterior energy. The mixing and mass transfer process of immiscible liquid–liquid two phases are intensified by gas agitation in the microchannels.

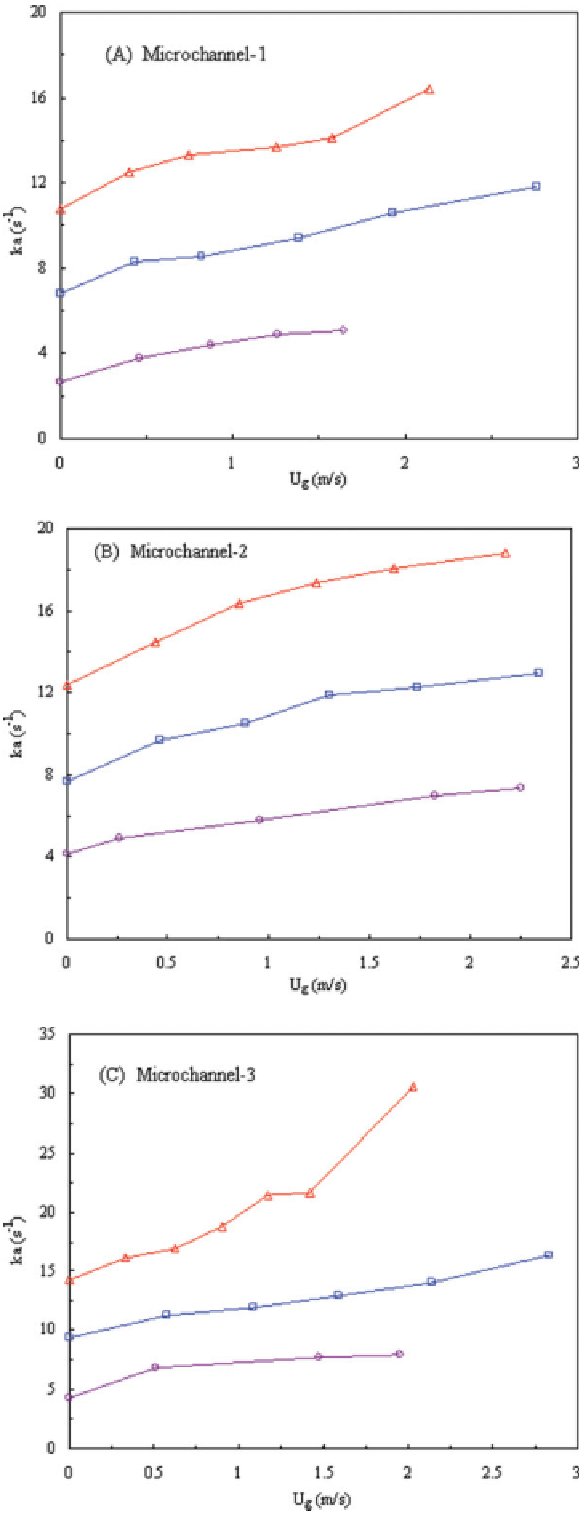

Figure 7. Effect of the gas phase flux on *ka* under different total liquid phase flux.

—○—: $U_{or} = 0.178$ m/s, $U_{aq} = 0.534$ m/s, $q = 1/3$, $Re_M = 203$. —□—: $U_{or} = 0.333$ m/s, $U_{aq} = 1$ m/s, $q = 1/3$, $Re_M = 381$. —△—: $U_{or} = 0.556$ m/s, $U_{aq} = 1.67$ m/s, $q = 1/3$, $Re_M = 635$. [Color figure can be viewed in the online issue, which is available at www.interscience.wiley.com.]

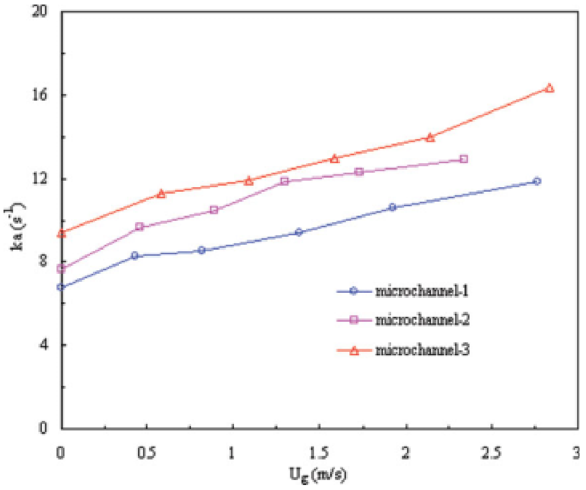

Figure 8. Effect of the microchannel structure on *ka* with gas agitation.

$U_{or} = 0.333$ m/s, $U_{aq} = 1$ m/s, $q = 1/3$, $Re_M = 381$. [Color figure can be viewed in the online issue, which is available at www.interscience.wiley.com.]

Effect of the microchannel structure on the values of ka with introducing gas

The effects of microchannel structure on the overall volumetric mean mass transfer coefficients with introducing gas are shown in Figures 8 and 9. The results demonstrate that the overall volumetric mean mass transfer coefficients in microchannel-3 are larger compared to those in microchannel-2 and microchannel-1 at the same flux, so it has the better mass transfer performance. This is attributed to the different dispersion performance to the immiscible liquid–liquid two phases by gas agitation in the three different microchannels. The gas–liquid–liquid three-phase flow patterns are almost determined by the inlet locations of the microchannel-1, however, they vary dramatically when the gas–liquid–liquid three-phase fluids flow through the 90° bends of the microchannel-2 and the microchannel-3. The centrifugal force[37] that is caused by abrupt varying of the flow direction plays an important role in the bends. The region of flow with a higher flow velocity tends to flow outwards while the slower flow at the top and bottom walls of the channel tends to flow inwards towards the bend under the action of centrifugal force. The slugs of aqueous phase are further broken up to smaller droplets by vertically impinging the channel wall when flowing through the microchannel bends successively under the condition of the centrifugal force effect (Figure 10a′), as a consequence, large interfacial mass transfer area and large surface renewal velocity can be obtained. At large total gas–liquid–liquid three phase flux, the effect of centrifugal force greatly exceeds the effect of interfacial tension in the microchannel bends. As shown in Figure 10b′, at large total liquid phase velocity and large gas velocity, when the fluids flow through every bend successively, the interface of immiscible liquid–liquid two phases becomes more unclear and the disturbance is more drastic with the joint action of gas agitation and microchannel bends, hence the interfacial mass transfer area and the surface renewal velocity are enlarged.

When flowing through the microchannel bends, even if the slugs of aqueous phase are not further broken up, the bends can also intensify the mass transfer process by gas agitation. The reason may be as follows: the aqueous phase slug has two symmetrical internal circulations in straight microchannel, but the slug is stretched, folded and distorted when flowing through the bends in the winding microchannel,[15,16] hence the symmetry of internal circulations is destroyed[38] and chaotic advection appears. The surface renewal velocity is enlarged due to the improvement of mixing performance in the aqueous phase slugs by chaotic advection.

The high dispersion of the immiscible liquid–liquid two phases can be obtained by the combined action of gas agitation and bends in the microchannels. The interfacial mass transfer area and the surface renewal velocity are all increased dramatically. The overall volumetric mean mass transfer coefficients are two-folds higher than those without gas agitating.

Effect of the gas inlet locations

Figure 11 demonstrates the dependency of the overall volumetric mean mass transfer coefficients on the gas inlet locations in the microchannel-3. From Figure 12, we can see that introducing gas from inlet-2 is better than from inlet-3 when the total liquid phase flux is relatively low, but the gas inlet locations do not impact on the overall volumetric mean mass transfer coefficients any more when the total liquid phases flux is larger. As the experimental observations, when introducing gas from inlet-2, the gas bubbles size is smaller and the frequency of producing bubbles is higher than those from inlet-3 (Figure 12), therefore, the gas can shear and disturb the interface of the immiscible liquid–liquid two phases more effectively, which results in an increase in the surface renewal velocity. This can be explained that the effect of bends is superior to other factors when the total

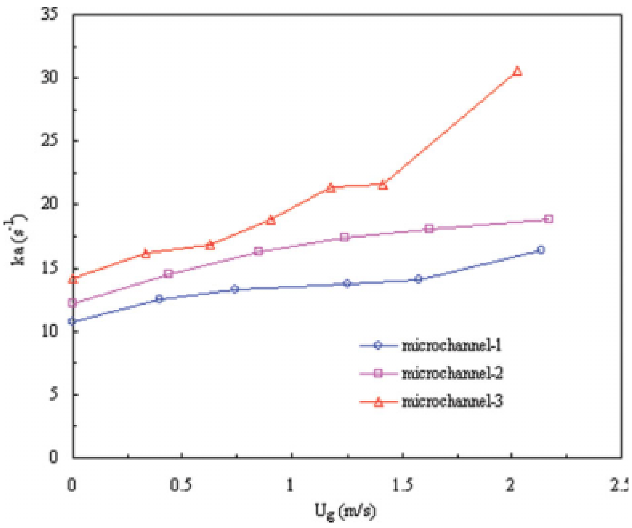

Figure 9. Effect of the microchannel structure on *ka* with gas agitation.

$U_{or} = 0.556$ m/s, $U_{aq} = 1.67$ m/s, $q = 1/3$, $Re_M = 635$. [Color figure can be viewed in the online issue, which is available at www.interscience.wiley.com.]

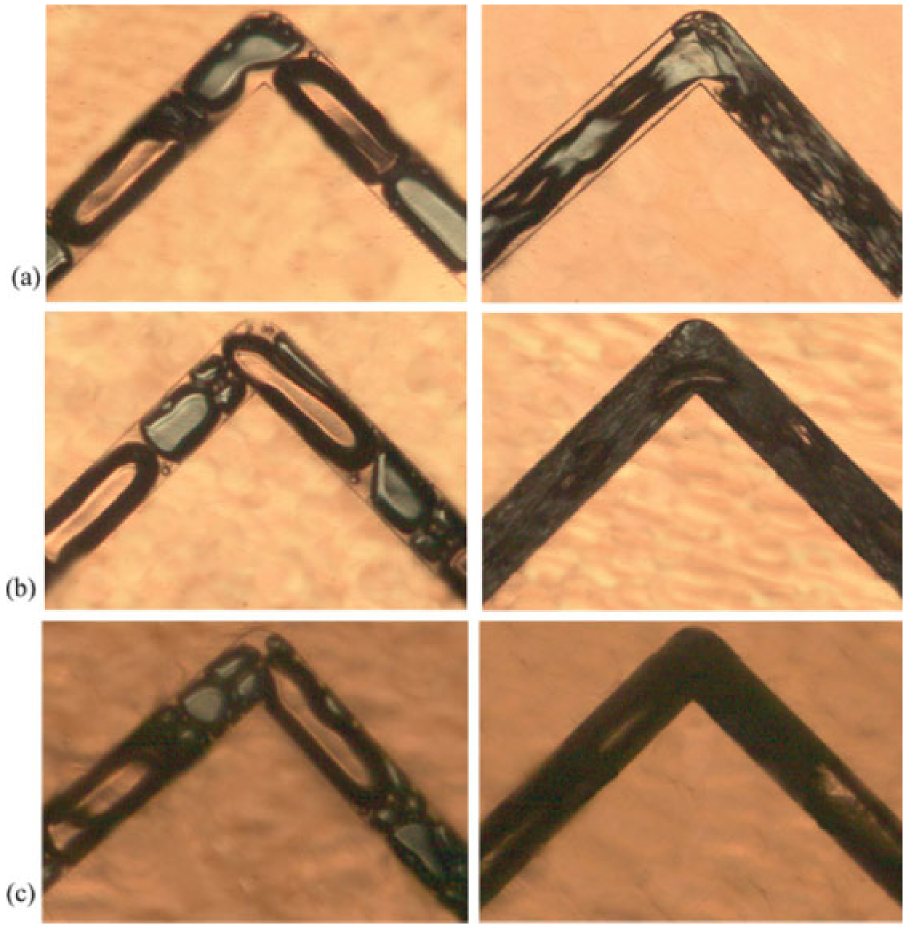

Figure 10. Effect of the microchannel-3 bends on the immiscible liquid–liquid two-phase dispersion with gas agitation at different total liquid phase velocity.

Flow state in 1st bend (a), 3rd bend (b), 5th bend (c). (a′) $U_{\mathrm{or}} = 0.056$ m/s, $U_{\mathrm{aq}} = 0.167$ m/s, $q = 1/3$, $Re_{\mathrm{M}} = 47.7$, $U_{\mathrm{g}} = 0.495$ m/s. (b′) $U_{\mathrm{or}} = 0.556$ m/s, $U_{\mathrm{aq}} = 1.67$ m/s, $q = 1/3$, $Re_{\mathrm{M}} = 635$, $U_{\mathrm{g}} = 1.99$ m/s.

liquid phase flux is larger, and the effect of the gas inlet locations can be neglected.

Correlation of the mass transfer data

The Re_{M} and microchannel structure are important operation parameters based on the frontal discussion. The effect of Re_{M} can be expressed as Re_{M}^{α} in the correlations according to previous work.[30] The mass transfer process between the immiscible liquid–liquid two phases can be intensified dramatically by gas agitation, so when predicting the volumetric mass transfer coefficients, the gas agitation must be considered as an important influence factor, which appears in the form of dimensionless number Re_{g} in the correlations. The factor $\exp(\beta Re_{\mathrm{g}})$ can be used to express the enhancement effect of gas agitation in the mass transfer process between the immiscible liquid–liquid two phases. When Re_{g} equals to zero, the factor $\exp(\beta Re_{\mathrm{g}})$ equals to 1, which represents the condition without gas agitation. The following correlations based on analysis of multiple linear regression are found to predict *ka* values well under the operation condition ($q = 1/3$, $Re_{\mathrm{M}} < 700$, $Re_{\mathrm{g}} < 100$).

For microchannel-1:

$$ka = 0.02325 Re_{\mathrm{M}}^{0.9475} \exp(0.0066 Re_{\mathrm{g}}) \tag{15}$$

For microchannel-2:

$$ka = 0.03085 Re_{\mathrm{M}}^{0.9318} \exp(0.0079 Re_{\mathrm{g}}) \tag{16}$$

For microchannel-3:

$$ka = 0.03501 Re_{\mathrm{M}}^{0.9326} \exp(0.0068 Re_{\mathrm{g}}) \tag{17}$$

Figure 13 demonstrates the experimental value of *ka* vs. the predicted value by Eqs. 15–17. The maximum relative deviation between the experimental and predicted values of *ka* does not exceed ±18%. From these correlations we can see the relative importance of the pertinent parameters on the mass transfer process in different structure microchannels.

Comparison with other kinds of liquid–liquid contactors

Table 2 lists typical overall volumetric mass transfer coefficients in the microchannel with and without gas agitation,

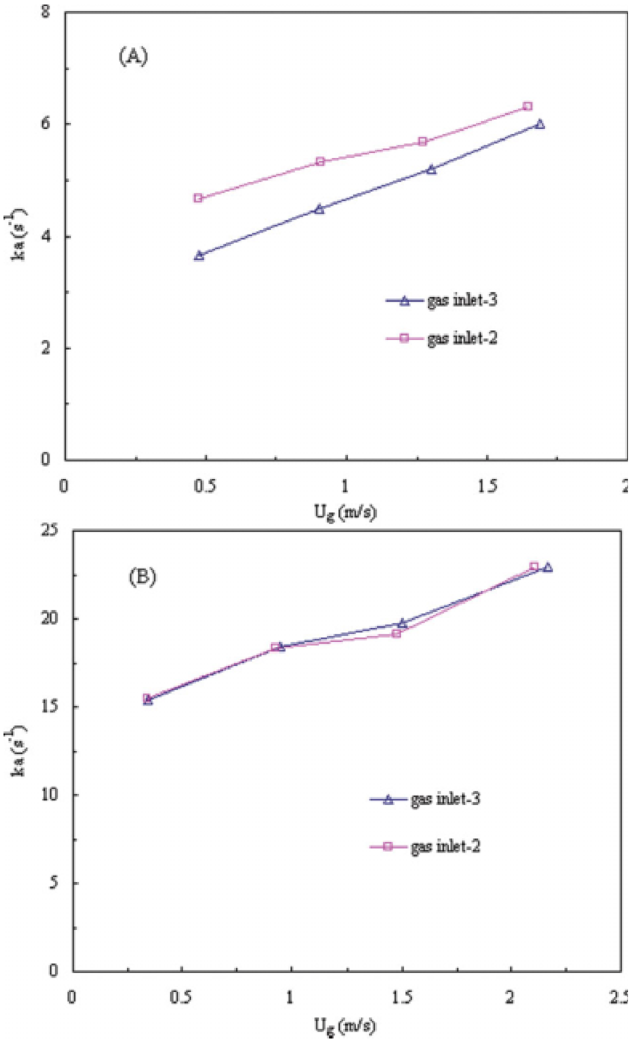

Figure 11. Effect of the gas inlet locations on *ka* at low total liquid phase flux in the microchannel-3.

(a) $U_{or} = 0.111$ m/s, $U_{aq} = 0.333$ m/s, $q = 1/3$, $Re_M = 127$. (b) $U_{or} = 0.5$ m/s, $U_{aq} = 1.5$ m/s, $q = 1/3$, $Re_M = 507$. [Color figure can be viewed in the online issue, which is available at www.interscience.wiley.com.]

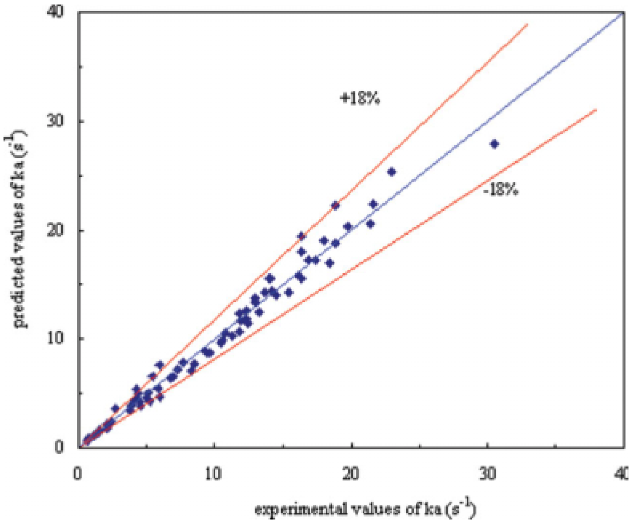

Figure 13. Experimental vs. predicted values of *ka*.

[Color figure can be viewed in the online issue, which is available at www.interscience.wiley.com.]

as well as those for some familiar liquid–liquid contactors. From Table 2 we can see the overall volumetric mass transfer coefficients obtained in the microchannels are more than two or three orders of magnitude higher than those liquid–liquid large scaled contactors.[32,39] Better mass transfer performance can be obtained in the microchannel, with the volume of microchannel smaller by two orders of magnitude. Therefore, significant mass transfer intensification implies that the adoption of microchannel is beneficial to many industrially important liquid–liquid mass transfer operations and reactions.

Conclusions

A new method which intensifies the mass transfer of two immiscible liquid–liquid phases in the microchannel by gas agitation is investigated. The effects of some pertinent parameters on the overall volumetric mean mass transfer coefficients have been studied. It is found that:

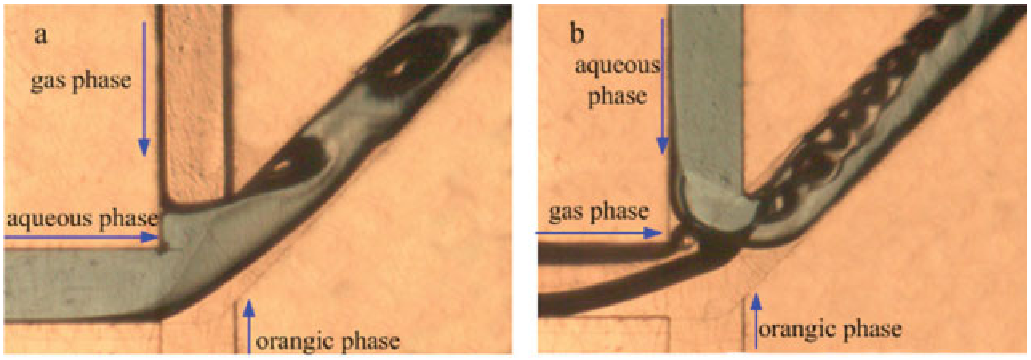

Figure 12. Effect of the gas inlet locations on the flow state.

(a) gas inlet-3; (b) gas inlet-2. $U_{or} = 0.278$ m/s, $U_{aq} = 0.833$ m/s, $q = 1/3$, $Re_M = 317$, $U_g = 0.758$ m/s.

Table 2. Comparison of the Values of *ka* in Different Liquid–Liquid Contactors

Type of Contactor	Chemical System	$k_a \times 10^4$ (s^{-1})
Agitated vessel[39]	Water-iodine-CCl_4	0.16–16.6
Rotary agitated column[39]	Water-acetone-toluene	0.2–1
Packed column[39]	Water-acetone-vinyl acetate	7.5–32
Cylindrical vessel with gas agitation[32]	Water-copper sulfate-LIX 860 (in kerosene)	33–75
Impinging streams contactor[39]	Water-acetic acid-kerosene	775–2500
Microchannel contactor (present work)	Water-acetic acid-TBP (in kerosene)	7700–306,000

1) The high dispersion of aqueous phase and organic phase in microhannel can be obtained by gas agitation. The dispersion performance is relevant to the gas velocity.

2) The microchannel structure does not affect the mass transfer process between the immiscible liquid–liquid two phases when Re_M are relatively low, but the influence is visible with Re_M increasing. The bends of microchannel can improve the mass transfer process.

3) In the microchannel, the mass transfer process between the immiscible liquid–liquid two phases can be intensified by gas agitation. In microscale space, the microchannel can be considered as microstirred tank, and the gas as microagitator. The overall volumetric mean mass transfer coefficients are two-folds higher than those without gas agitating.

4) The gas inlet locations impact on the overall volumetric mean mass transfer coefficients at low total liquid phase flux, but the gas inlet locations do not impact on the overall volumetric mean mass transfer coefficients at high total liquid phase flux.

5) Compared with the other liquid–liquid contactors reported on the overall volumetric mass transfer coefficients, the microchannel contactor can significantly enhance the mass transfer process.

Acknowledgments

The work reported in this article was financially supported by research grants from the National Natural Science Foundation of China and China National Petroleum Corporation (Nos. 20490208 and 20676129), 863 Projects (2006AA05Z233, 2007AA030206) and Open Fund of State Key Laboratory of Explosion Science and Technology, Beijing Institute of Technology (KFJJ06-1) for this work.

Notation

a = interfacial area, m^2/m^3
A = cross-sectional area of microchannel, m^2
C_{aq} = concentration of aqueous phase, mol/l
$C^*_{or,i}$ = equilibrium concentration of the solutes in the inlet organic phase corresponding to the actual inlet concentration of the solutes in the aqueous phase, mol/l
$C_{or,o}$ = concentration of the solute in the organic phase after phases separating, mol/l
$C^*_{or,o}$ = equilibrium concentration of the solutes in the outlet organic phase corresponding to the actual outlet concentration of the solutes in the aqueous phase, mol/l
D_H = hydraulic diameter of microchannel, m
k = overall mean mass transfer coefficient, m/s
ka = overall mean mass transfer coefficient, 1/s
ka_i = overall volumetric mean mass transfer coefficient in the microchannel-i (i 1, 2 , 3), 1/s
m = partition coefficient of solute between aqueous and organic phases
q = volume flux ratio of organic phase to aqueous phase
Q_{aq} = aqueous phase volume flow rate, m^3/s
Q_g = gas volume flow rate, m^3/s
Q_{or} = organic phase volume flow rate, m^3/s
Re = Reynolds number of fluid
Re_M = mixture Reynolds number of the immiscible liquid–liquid two phases
Re_g = Reynolds number of gas phase
t = superficial residence time in microchannel, s
U_{aq} = aqueous phase superficial velocity, m/s
U_M = total liquid phase superficial velocity, m/s
U_{or} = organic phase superficial velocity, m/s
U_g = gas superficial velocity, m/s
V = volume of microchannel, m^3

Greek letters

α = function coefficient of mixture Reynolds number of the immiscible liquid–liquid two phases
β = function coefficient of gas agitation
μ = viscosity, Pa·s
ρ = mass density, kg/m^3
φ = volume fraction

Subscripts

aq = aqueous phase
g = gas phase
M = mixture of the immiscible liquid–liquid two phases
or = organic phase
1 = microchannel-1
2 = microchannel-2
3 = microchannel-3

Literature Cited

1. Hessel V, Lowe H. Microchemical engineering: Components, plant concepts user acceptance - Part I. *Chem Eng Technol.* 2003;26:3–24.
2. Chen GW, Yuan Q, Li HQ, Li SL. CO selective oxidation in a microchannel reactor for PEM fuel cell. *Chem Eng J.* 2004;101: 101–106.
3. Jahnisch K, Hessel V, Lowe H, Baerns M. Chemistry in microstructured reactors. *Angew Chem Int Ed.* 2004;43:406–446.
4. Jahnisch K, Baerns M, Hessel V, Ehrfeld W, Haverkamp V, Lowe H, Wille C, Guber A. Direct fluorination of toluene using elemental fluorine in gas/liquid microreactors. *J Fluorine Chem.* 2000;105: 117–128.
5. Besser RS, Ouyang X, Surangalikar H. Hydrocarbon hydrogenation and dehydrogenation reactions in microfabricated catalytic reactors. *Chem Eng Sci.* 2003;58:19–26.
6. Kestenbaum H, de Oliveira AL, Schmidt W, Schuth F, Ehrfeld W, Gebauer K, Lowe H, Richter T, Lebiedz D, Untiedt I, Zuchner H. Silver-catalyzed oxidation of ethylene to ethylene oxide in a microreaction system. *Ind Eng Chem Res.* 2002;41:710–719.
7. Zanfir M, Gavriilidis A, Wille C, Hessel V. Carbon dioxide absorption in a falling film microstructured reactor: experiments and modeling. *Ind Eng Chem Res.* 2005;44:1742–1751.
8. Burns JR, Ramshaw C. A microreactor for the nitration of benzene and toluene. *Chem Eng Commun.* 2002;189:1611–1628.
9. SalimiMoosavi H, Tang T, Harrison DJ. Electroosmotic pumping of organic solvents and reagents in microfabricated reactor chips. *J Am Chem Soc.* 1997;119:8716–8717.
10. Ying Y, Chen GW, Zhao YC, Li SL, Yuan Q. A high throughput methodology for continuous preparation of monodispersed nanocrystals in microfluidic reactors. *Chem Eng J.* 2008;135:209–215.

11. TeGrotenhuis WE, Cameron RJ, Butcher MG, Martin PM, Wegeng RS. Microchannel devices for efficient contacting of liquids in solvent extraction. *Sep Sci Technol.* 1999;34:951–974.
12. Wong SH, Ward MCL, Wharton CW. Micro T-mixer as a rapid mixing micromixer. *Sensor Actuators B.* 2004;100:359–379.
13. Jen CP, Wu CY, Lin YC, Wu CY. Design and simulation of the micromixer with chaotic advection in twisted microchannels. *Lab Chip.* 2003;3:77–81.
14. Yang Z, Matsumoto S, Goto H, Matsumoto M, Maeda R. Ultrasonic micromixer for microfluidic systems. *Sensor Actuators A.* 2001;93: 266–272.
15. Bringer MR, Gerdts CJ, Song H, Tice JD, Ismagilov RF. Microfluidic systems for chemical kinetics that rely on chaotic mixing in droplets. *Philos Trans R Soc A.* 2004;362:1087–1104.
16. Tice JD, Song H, Lyon AD, Ismagilov RF. Formation of droplets and mixing in multiphase microfluidics at low values of the Reynolds and the capillary numbers. *Langmuir.* 2003;19:9127–9133.
17. Matsuyama K, Tanthapanichakoon W, Aoki N, Mae K. Operation of microfluidic liquid slug formation and slug design for kinetics measurement. *Chem Eng Sci.* 2007;62:5133–5136.
18. Gunther A, Jhunjhunwala M, Thalmann M, Schmidt MA, Jensen KF. Micromixing of miscible liquids in segmented gas-liquid flow. *Langmuir.* 2005;21:1547–1555.
19. Gunther A, Khan SA, Thalmann M, Trachsel F, Jensen KF. Transport and reaction in microscale segmented gas-liquid flow. *Lab Chip.* 2004;4:278–286.
20. Khan SA, Gunther A, Schmidt MA, Jensen KF. Microfluidic synthesis of colloidal silica. *Langmuir.* 2004;20:8604–8611.
21. Song H, Chen DL, Ismagilov RF. Reactions in droplets in microfluidic channels. *Angew Chem Int Ed.* 2006;45:7336–7356.
22. Chan EM, Alivisatos AP, Mathies RA. High-temperature microfluidic synthesis of CdSe nanocrystals in nanoliter droplets. *J Am Chem Soc.* 2005;127:13854–13861.
23. Song H, Ismagilov RF. Millisecond kinetics on a microfluidic chip using nanoliters of reagents. *J Am Chem Soc.* 2003;125:14613–14619.
24. Zheng B, Tice JD, Roach LS, Ismagilov RF. A droplet-based, composite PDMS/glass capillary microfluidic system for evaluating protein crystallization conditions by microbatch and vapor-diffusion methods with on-chip X-ray diffraction. *Angew Chem Int Ed.* 2004; 43:2508–2511.
25. Khan SA, Jensen KF. Microfluidic synthesis of titania shells on colloidal silica. *Adv Mater.* 2007;19:2556–2560.
26. Triplett KA, Ghiaasiaan SM, Abdel-Khalik SI, Sadowski DL. Gas-liquid two-phase flow in microchannels, Part I: two-phase flow patterns. *Int J Multiphase Flow.* 1999;25:377–394.
27. Triplett KA, Ghiaasiaan SM, Abdel-Khalik SI, LeMouel A, McCord BN. Gas-liquid two-phase flow in microchannels, Part II: void fraction and pressure drop. *Int J Multiphase Flow.* 1999;25:395–410.
28. Yue J, Chen GW, Yuan Q, Luo LG, Gonthier Y. Hydrodynamics and mass transfer characteristics in gas-liquid flow through a rectangular microchannel. *Chem Eng Sci.* 2007;62:2096–2108.
29. Zhao YC, Chen GW, Yuan Q. Liquid-liquid two-phase flow patterns in a rectangular microchannel. *AIChE J.* 2006;52:4052–4060.
30. Zhao YC, Chen GW, Yuan Q. Liquid-liquid two-phase mass transfer in the T-junction microchannels. *AIChE J.* 2007;53:3042–3053.
31. Galkin GP, Goriainov NE, Tikhomirov VB. The mechanism of distribution of liquids in a plate extractor. *J Nucl Energy.* 1961;14: 132–133.
32. Doungdeethaveeratana D, Sohn HY. The kinetics of extraction in a novel solvent extraction process with bottom gas injection without moving parts. *Hydrometallurgy.* 1998;49:229–254.
33. Lu S, Mi ZT, Wang YQ, Wang L. Experimental investigation and simulation of a gas-agitated sieve plate column. *Chem Eng Technol.* 2004;27:903–908.
34. Dreyfus R, Tabeling P, Willaime H. Ordered and disordered patterns in two-phase flows in microchannels. *Phys Rev Lett.* 2003;90:144505.
35. Guillot P, Colin A. Stability of parallel flows in a microchannel after a T junction. *Phys Rev E.* 2005;72:066301.
36. Fries DA, Waelchli S, Von Rohr PR. Gas-liquid two-phase flow in meandering microchannels. *Chem Eng J.* 2008;135:S37–S45.
37. Ahn YC, Jung WG, Chen ZP. Optical sectioning for microfluidics: secondary flow and mixing in a meandering microchannel. *Lab Chip.* 2008;8:125–133.
38. Song H, Tice JD, Ismagilov RF. A microfluidic system for controlling reaction networks in time. *Angew Chem Int Ed.* 2003;42:768–772.
39. Dehkordi AM. Novel type of impinging streams contactor for liquid-liquid extraction. *Ind Eng Chem Res.* 2001;40:681–688.

Manuscript received July 7, 2008, and revision received Nov. 17, 2008.